

Article

Variable-Coefficient Dynamic Modeling Method for a Ball Screw Feed System in the No-Extra-Load Running State

Huijie Zhang ^{1,*}, Jun Zha ¹, Chao Du ², Hui Liu ¹, Yang Li ¹ and Dun Lv ¹

¹ Collaborative Innovation Center of High-End Manufacturing Equipment, Xi'an Jiaotong University, Xi'an 710054, China

² Shaanxi Fast Gear Co., Ltd., Xi'an 710077, China

* Correspondence: zhanghuijie@xjtu.edu.cn

Abstract: In a ball screw feed system of high-speed/high-acceleration machine tools, large frictional and inertial forces may change the real contact state of the kinematic joints, resulting in changes in the contact and transmission stiffnesses and, hence, changes in the dynamic characteristics of the system. In this study, a variable-coefficient dynamic modeling method for a ball screw feed system is proposed, considering the influence of changes in the no-extra-load running states, such as position, speed, and acceleration. Based on Timoshenko beam elements with two nodes and four DOFs, an equivalent dynamic model of a ball screw feed system is established using the hybrid element method. The expression for the equivalent axial stiffness of individual kinematic joints is derived, considering the influence of the feed speed/acceleration under the no-extra-load running state of the system. In addition, the stiffness and mass of the screw shafts on both sides of the screw nut are calculated, considering the influence of the system's feed position. Hence, we obtain the total stiffness and mass of the system in the no-extra-load running state and analyze the natural frequency. Finally, we conduct validation experiments on a ball screw feed system of a large gantry-type machine tool with different no-extra-load running states.

Keywords: ball screw feed system; variable coefficient; dynamic modeling method; kinematic joints; machine tool



Citation: Zhang, H.; Zha, J.; Du, C.; Liu, H.; Li, Y.; Lv, D.

Variable-Coefficient Dynamic Modeling Method for a Ball Screw Feed System in the No-Extra-Load Running State. *Processes* **2023**, *11*, 793. <https://doi.org/10.3390/pr11030793>

Academic Editor: Udo Fritsching

Received: 8 February 2023

Revised: 28 February 2023

Accepted: 3 March 2023

Published: 7 March 2023



Copyright: © 2023 by the authors. Licensee MDPI, Basel, Switzerland. This article is an open access article distributed under the terms and conditions of the Creative Commons Attribution (CC BY) license (<https://creativecommons.org/licenses/by/4.0/>).

1. Introduction

The ball screw feed system is the most common transmission mechanism in machine tools; its dynamics are related to the dynamic characteristics of the mechanical structure, the control performance of the system, and the matching performance between them [1–3]. System dynamics directly influence the position accuracy [4–6], machining accuracy [7,8] and stability of the cutting process [9–11]. In addition, a suitable dynamic model of the feed system is a prerequisite for designing the control system of a high-performance machine tool [12]. The stiffness of the individual kinematic joints (screw nut joints and bearing joints) of the feed system and the tension/compression and torque stiffnesses of the screw shaft on both sides of the nuts are the most significant factors affecting the dynamics of the system. Therefore, the accuracy of the kinematic joint parameters is crucial for the dynamic model of the ball screw feed system.

Researchers have studied the dynamic characteristics of a ball screw feed system using the lumped parameter method [13], the hybrid element method [14,15], and the finite element method [16–18]. Feng et al. [19] used the lumped parameter method to analyze the influence of the preload of screw nut joints on the dynamic performance of the screw nut system. Zhou et al. established a hybrid dynamic model of a ball screw feed system [20]; they analyzed the variation in the dynamic characteristics of the screw shaft with different axial stiffnesses of the bearing joints. Mi et al. [21] explored the variation in dynamic stiffness at the tool point with a series of preloads applied on the screw nut joint and discovered that the preload could significantly influence the stiffness in the transmission direction.

Based on signals acquired from an embedded sensing system on a ball screw structure, Feng et al. [22] diagnosed the preloads of a ball screw nut under different conditions using the support vector machine method and monitored the fitness of a ball screw. A recently proposed method applied by Tsai et al. [23] provided an economic means of detecting the preload loss of ball screws. All the above studies provided a deeper understanding of the characteristics and dynamic modeling of a ball screw feed system.

Currently, high-speed and high-acceleration machine tools are widely used [24,25]. Moreover, a large-scale NC machine tool is required for manufacturing large workpieces. However, the inertial force derived from the acceleration and the friction force derived from the velocity [26–31] may change the real contact state of the kinematic joints, resulting in changes in the contact and transmission stiffnesses, which will further affect the dynamic characteristics of the system. For the ball screw feed system of a large-scale machine tool, the position of the screw nut joints will change significantly when the moving component moves along its entire stroke. Therefore, the tension/compression and torsion stiffnesses of the screw shaft on both sides of the screw nut joints change. Thus, the transmission stiffness of the system varies and affects the dynamic characteristics of the system.

In this study, a variable-coefficient dynamic modeling method for a ball screw feed system is proposed, considering the influence of changes in the no-extra-load running state of the system. Based on Timoshenko beam elements with two nodes and four DOFs, an equivalent dynamic model of a ball screw feed system is established using the hybrid element method. The expression for the equivalent axial stiffness of individual kinematic joints is derived, considering the influence of the system feed speed/acceleration. The stiffness of the screw shafts is calculated, considering the influence of the system feed position. Hence, we obtain the total stiffness of the system in a no-extra-load running state and analyze the natural frequency. We perform experiments on the ball screw feed system of a large gantry-type machine tool to verify the proposed dynamic model.

2. Materials and Methods

2.1. Equivalent Dynamic Model

As a typical transmission unit with high precision and efficiency, a ball screw feed system is widely used in various types of machine tools. It primarily comprises a coupling and servo motor, bearing units, a screw shaft, a screw nut, a linear guide and slider, and a worktable, as shown in Figure 1. Among the six directions of freedom (TX/TY/TZ translational degrees of freedom and RX/RZ rotational degrees of freedom) for workability, the non-feed directions of freedom (TY/TZ/RX/RZ) of the worktable are constrained by a linear guide with high stiffness. The worktable in the TX direction (the transmission direction) is constrained by the screw nut, the bearing units, the screw shaft, the bearing housing, and the screw nut bracket. The stiffness in the transmission direction is less than that in the non-feed direction because of the kinematic joints and the flexible components. The contact stiffness of the kinematic joints is affected by the inertial and frictional forces, which originate from acceleration and speed, respectively. Consequently, the system dynamics primarily depend on the transmission stiffness, and the associated dynamic characteristics of the system directly affect the machining quality [7,8,32] and limit the bandwidth of the control system [12,33]. Therefore, the dynamic modeling method of a ball screw feed system in the transmission direction with the system in the no-extra-load running state is discussed.

In Figure 2,

m_t is the total mass of the system; a_t and v_t are the feed acceleration and the speed of the system, respectively; x_{vari} is the distance between the screw nut and the front-end support-bearing units, and L_{fix} is the screw shaft length between the front-end support-bearing units and the rear-end support-bearing units.

$k_{1bx}(F_{as-b}, f(a_t, v_t))$, $k_{2bx}(F_{as-b}, f(a_t, v_t))$, and $k_{nut}(P_{Ca}, f(a_t, v_t))$ are the equivalent axial stiffnesses of the front-end support-bearing unit joints, the rear-end support-bearing unit joints, and the screw nut joints, respectively. They are the functions of speed, acceleration, etc.

① and ② are Timoshenko beam elements; 1, 2, 3, and 4 are the node numbers. Node 2 moves along the X direction. The position changes of node 2 can reflect the variations in the length of the screw shafts on both sides of the screw nut, which further influences the stiffness and mass matrix of the system.

2.2. Variable-Coefficient Dynamic Equation

As described in Section 2.1, the running state leads to variations in system stiffness and mass matrix. Therefore, in view of the equivalent dynamic model and the D'Alembert principle, a variable-coefficient dynamic equation of a ball screw feed system can be derived as follows:

$$[M(x_{vari})]\{\ddot{q}\} + [C]\{\dot{q}\} + [K(f(a_t, v_t), P_{Ca}, F_{as-b}, x_{vari}, L_{fix})]\{q\} = [0] \tag{1}$$

where

$[M(x_{vari})]$ is the total mass matrix of the ball screw feed system, $[C]$ is the total damping matrix of the ball screw feed system, and $[K(f(a_t, v_t), P_{Ca}, F_{as-b}, x_{vari}, L_{fix})]$ is the total stiffness matrix of the ball screw feed system. The total stiffness matrix is primarily determined by the equivalent stiffness of the screw nut joints, the front-end support-bearing units, the rear-end support-bearing units, and the screw shafts. In this study, only the natural frequency of the ball screw feed system was considered; hence, the damping coefficient $[C]$ was neglected.

2.3. Determination of the Variable-Coefficient of the Dynamic Equation

2.3.1. Stiffness and Mass Matrices of the Equivalent Beam Element

As described in Section 2.1, considering the influence of the worktable position and the screw pitch, the stiffness matrix of the equivalent beam element ① can be obtained as follows:

$$K^1 = \begin{bmatrix} K_{11}^1 & K_{12}^1 \\ K_{21}^1 & K_{22}^1 \end{bmatrix} \tag{2}$$

where

$$K_{11}^1 = K_{22}^1 = \begin{bmatrix} \frac{1}{\frac{E_{ss} \cdot A_{ss}}{x_{vari}} + \left(\frac{2\pi}{p_{ss}}\right)^2 \frac{G_{ss} \cdot I_{pss}}{x_{vari}}} & 0 \\ 0 & \frac{G_{ss} \cdot I_{pss}}{x_{vari}} \end{bmatrix} \tag{3}$$

$$K_{12}^1 = K_{21}^1 = \begin{bmatrix} -\frac{1}{\frac{E_{ss} \cdot A_{ss}}{x_{vari}} + \left(\frac{2\pi}{p_{ss}}\right)^2 \frac{G_{ss} \cdot I_{pss}}{x_{vari}}} & 0 \\ 0 & -\frac{G_{ss} \cdot I_{pss}}{x_{vari}} \end{bmatrix} \tag{4}$$

where

E_{ss} and G_{ss} are Young's elastic modulus and shear modulus, respectively, I_{pss} is the polar moment of inertia for the beam element; and A_{ss} and p_{ss} are the cross-sectional area

and the pitch of the screw shaft, respectively. Similarly, for element ②, the stiffness matrix can be derived [31] using Equation (5).

$$K^2 = \begin{bmatrix} K_{22}^2 & K_{32}^2 \\ K_{32}^2 & K_{33}^2 \end{bmatrix} = \begin{bmatrix} \frac{E_{ss} \cdot A_{ss}}{L_{fix} - x_{vari}} & 0 \\ 0 & 0 \\ -\frac{E_{ss} \cdot A_{ss}}{L_{fix} - x_{vari}} & 0 \\ 0 & 0 \end{bmatrix} \begin{bmatrix} -\frac{E_{ss} \cdot A_{ss}}{L_{fix} - x_{vari}} & 0 \\ 0 & 0 \\ \frac{E_{ss} \cdot A_{ss}}{L_{fix} - x_{vari}} & 0 \\ 0 & 0 \end{bmatrix} \quad (5)$$

As described in Section 2.1, the mass matrices of the equivalent Timoshenko beam elements ① and ② vary with the worktable position and are determined [34] by Equations (6) and (7).

$$M^1 = \begin{bmatrix} M_{11}^1 & M_{12}^1 \\ M_{21}^1 & M_{22}^1 \end{bmatrix} = \rho_{ss} A_{ess} x_{vari} \begin{bmatrix} \frac{1}{3} & 0 \\ 0 & \frac{I_{\rho ss}}{3A_{ess}} \\ \frac{1}{6} & 0 \\ 0 & \frac{I_{\rho ss}}{6A_{ess}} \end{bmatrix} \begin{bmatrix} \frac{1}{6} & 0 \\ 0 & \frac{I_{\rho ss}}{6A_{ess}} \\ \frac{1}{3} & 0 \\ 0 & \frac{I_{\rho ss}}{3A_{ess}} \end{bmatrix} \quad (6)$$

$$M^2 = \begin{bmatrix} M_{22}^2 & M_{23}^2 \\ M_{32}^2 & M_{33}^2 \end{bmatrix} = \rho_{ss} A_{ess} (L_{fix} - x_{vari}) \begin{bmatrix} \frac{1}{3} & 0 \\ 0 & \frac{I_{\rho ss}}{3A_{ess}} \\ \frac{1}{6} & 0 \\ 0 & \frac{I_{\rho ss}}{6A_{ess}} \end{bmatrix} \begin{bmatrix} \frac{1}{6} & 0 \\ 0 & \frac{I_{\rho ss}}{6A_{ess}} \\ \frac{1}{3} & 0 \\ 0 & \frac{I_{\rho ss}}{3A_{ess}} \end{bmatrix} \quad (7)$$

where

ρ_{ss} denotes the material density of the ball screw shaft and A_{ess} is the cross-sectional area of the equivalent Timoshenko beam element.

2.3.2. Equivalent Axial Stiffness of the Screw Nut Joints

Figure 3 shows a cross-sectional view of a typical gasket-type double-nut ball screw joint. The positive and negative rotations of the screw shaft are converted to the reciprocating movement of the worktable because of the direct link between the screw nut and the worktable.

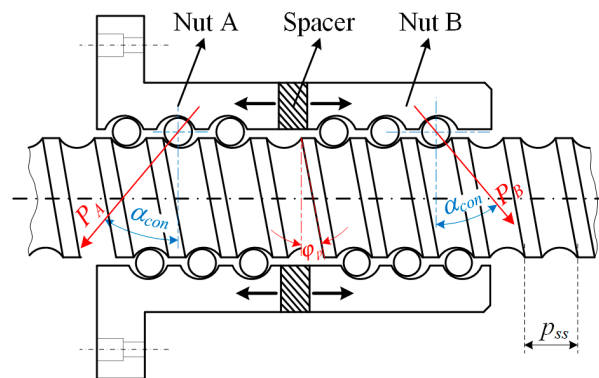


Figure 3. Cross-sectional view of a typical gasket-type double-nut ball screw joint.

Suppose that the worktable moves along the negative X direction with feed speed v_t and feed acceleration a_t , the frictional and inertial forces applied to the screw nut joints. Assuming that elastic deformation only exists on the ball between the screw shaft and the screw nuts [30,31], which can be calculated using the Hertz contact theory [35], the equivalent axial stiffness of the screw nut joints, considering the feed speed and the feed acceleration, can be obtained by Equation (8).

$$\begin{cases} k_{nut}(P_{Ca}, f(a_t, v_t)) = \frac{3}{2} K_h^{2/3} \cdot (P_{Ca} + f(a_t, v_t))^{1/3} \cdot \left(\sin^5 \alpha_{con} \cdot \cos^5 \varphi_p \cdot \left(\frac{i_{sn} \cdot \pi \cdot d_0}{d_{sb} \cdot \cos \varphi_p} \right)^2 \right)^{1/3} \cdot c_{wn} \\ P_{Ca} = P_d \cdot C_p \end{cases} \quad (8)$$

where

P_d and C_p are the rated dynamic load of the screw nut joints and the coefficient of the rated dynamic load of the screw nut joints, respectively. P_{Ca} is the initial preload of double nuts, α_{con} and φ_p are the contact angles between the ball and race and the lead angle of the screw shaft, respectively. i_{sn} is the total number of load-bearing rings of the single nut and d_0 and d_{sb} are the nominal diameter of the screw shaft and the diameter of the ball in the screw nut joints, respectively. c_{wn} is the coefficient of the equivalent axial stiffness of the screw nut joints and K_h is the Hertz contact coefficient. It is determined by the contact shape of the screw nuts and the material properties of the ball [36,37].

2.3.3. Equivalent Axial Stiffness of the Bearing Joints

Figure 4 shows the assembly structure of the support-bearing units on both ends of a feed system.

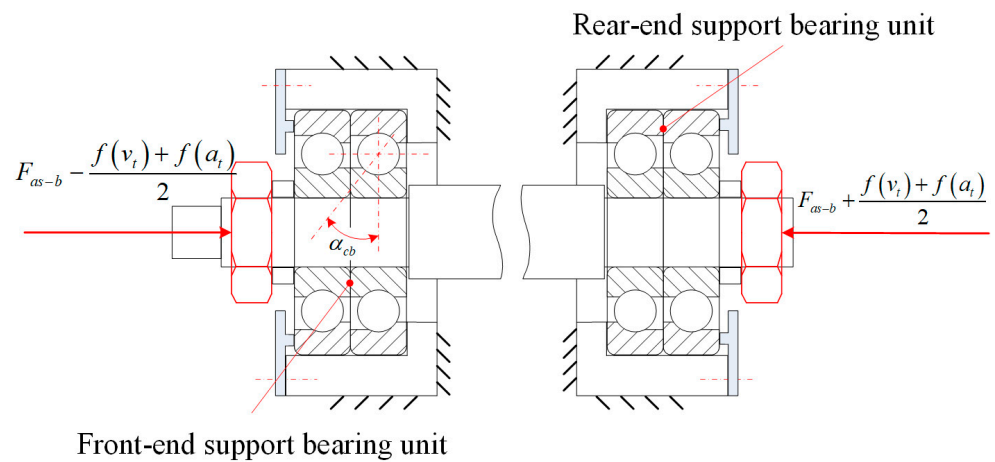


Figure 4. Assembly structure of the support bearing units of a feed system.

Assume that the worktable moves along the negative X direction with the feed speed v_t and the friction force applied on both bearings has the same value but an opposite direction; the value of single-ended is $f(v_t)/2$. Similarly, suppose that the worktable moves along the negative X direction with the feed acceleration a_t and the inertial force applied on both bearings has the same value but an opposite direction; the value of single-ended is $f(a_t)/2$. Assuming that elastic deformation exists only on the ball of the bearing joints (Figure 4), the equivalent axial stiffness of the front-end support bearing unit and rear-end support-bearing unit [30,31,35] can be derived using Equations (9) and (10).

$$k_{1bx}(F_{as-b}, f(v_t, a_t)) = \begin{cases} \frac{3}{2} K_h^{2/3} \cdot \left(F_{as-b} - \frac{f(v_t) + f(a_t)}{2} \right)^{1/3} \cdot \left(\sin^5 \alpha_{cb} \cdot (i_b \cdot n_b)^2 \right)^{1/3} \cdot c_{wb} \\ 0 \end{cases} \quad (9)$$

$$k_{2bx}(F_{as-b}, f(v_t, a_t)) = \frac{3}{2} K_h^{2/3} \cdot \left(F_{as-b} + \frac{f(v_t) + f(a_t)}{2} \right)^{1/3} \cdot \left(\sin^5 \alpha_{cb} \cdot (i_b \cdot n_b)^2 \right)^{1/3} \cdot c_{wb} \quad (10)$$

where F_{as-b} is the ball screw tension force, α_{cb} is the contact angle of the bearing joints, i_b and n_b are the number of single-ended load-bearing units and the ball number of a bearing, respectively. c_{wb} is the coefficient of the equivalent axial stiffness of the bearing joints.

2.3.4. Total Stiffness and Mass Matrices of the System Based on Changes in the No-Extra-Load Running State

According to the stiffness matrix of the equivalent beam element in Section 2.3.1 and the equivalent axial stiffness of the kinematic joints in Sections 2.3.2 and 2.3.3, the total stiffness matrix of the system can be derived using Equation (11), with changes in the no-extra-load running state [34].

$$K = \begin{bmatrix} K_{11}^1 + K_{11}^{1bx} & K_{12}^1 & 0 & 0 \\ K_{21}^1 & K_{22}^1 + K_{22}^2 + K_{22}^{nut} & K_{23}^2 & K_{24}^{nut} \\ 0 & K_{32}^2 & K_{33}^2 + K_{33}^{2bx} & 0 \\ 0 & K_{42}^{nut} & 0 & K_{44}^{nut} \end{bmatrix} \tag{11}$$

where

$$\begin{aligned} K_{11}^{1bx} &= \begin{bmatrix} k_{1bx}(F_{as-b}, f(v_t, a_t)) & 0 \\ 0 & 0 \end{bmatrix} \\ K_{33}^{2bx} &= \begin{bmatrix} k_{2bx}(F_{as-b}, f(v_t, a_t)) & 0 \\ 0 & 0 \end{bmatrix} \\ K_{22}^{nut} = K_{44}^{nut} &= \begin{bmatrix} k_{nut}(f(v_t, a_t), P_{Ca}) & 0 \\ 0 & 0 \end{bmatrix} \\ K_{24}^{nut} = K_{42}^{nut} &= \begin{bmatrix} -k_{nut}(f(v_t, a_t), P_{Ca}) & 0 \\ 0 & 0 \end{bmatrix} \end{aligned} \tag{12}$$

Similarly, the total mass matrix of the system, with changes in the no-extra-load running state, is expressed as follows:

$$M = \begin{bmatrix} M_{11}^1 & M_{12}^1 & 0 & 0 \\ M_{21}^1 & M_{22}^1 + M_{22}^2 & M_{23}^2 & 0 \\ 0 & M_{32}^2 & M_{33}^2 & 0 \\ 0 & 0 & 0 & M_{44}^t \end{bmatrix} \tag{13}$$

where

$$M_{44}^t = \begin{bmatrix} m_t & 0 \\ 0 & 0 \end{bmatrix} \tag{14}$$

3. Dynamic Measurement of a Ball Screw Feed System in Different Running States

The experiments on a ball screw feed worktable system of a large gantry-type machine tool driven in different running states was performed to verify the proposed dynamic model. The worktable was driven by a ball screw feed system BNFN8016S-5), and the ball screw support-bearing units (NSK 60TAC 120B) were used at both ends of the screw shaft in the form of a DT structure. Table 1 lists the parameters of the experimental device for the ball screw feed system.

Table 1. The parameters of the experimental device.

Parameter	Value	Parameter	Value	Parameter	Value
F_{as-b}/kN	1.70	P_d/kN	163.4	A_{ess}/m^2	4.8×10^{-3}
$\alpha_{cb}/^\circ$	60	C_p	0.10	A_{ss}/m^2	4.2×10^{-3}
i_b/n_b	2/29	$\alpha_{con}/^\circ$	60	$E_{ss}/(\text{N}/\text{m}^2)$	2.1×10^{11}
c_{wb}/c_{wn}	0.8	$\varphi_p/^\circ$	3.643	$G_{ss}/(\text{N}/\text{m}^2)$	0.8×10^{11}
m_t/kg	7400	i_{sn}	2.5	$\rho_{ss}/(\text{kg}/\text{m}^3)$	7.85×10^3
d_0/mm	80	d_{sb}/mm	9.525	$I_{\rho_{ss}}/\text{m}^4$	3.6×10^{-6}
p_{ss}/mm	16	L_{fix}/m	5.3		

The dynamic characteristics of the ball screw feed system were tested using the LMS Test.Lab SCM05, where the screw nut was located in the middle of the screw shaft ($x_{vari} = 2.65$ m); five tests were performed, as shown in Figure 5. Acceleration sensors with three directions were installed on the four corners of the worktable. The excitation point was exerted on one side of the worktable. The frequency bandwidth was 512 Hz and the number of spectral lines was 1024. The type, serial number, and sensitivity of the hammer were 086D50, SN 36973, and 0.23 mV/N, respectively. Table 2 lists the types, the serial numbers of the acceleration sensors, and the sensitivities of the acceleration sensors in the X, Y, and Z directions.

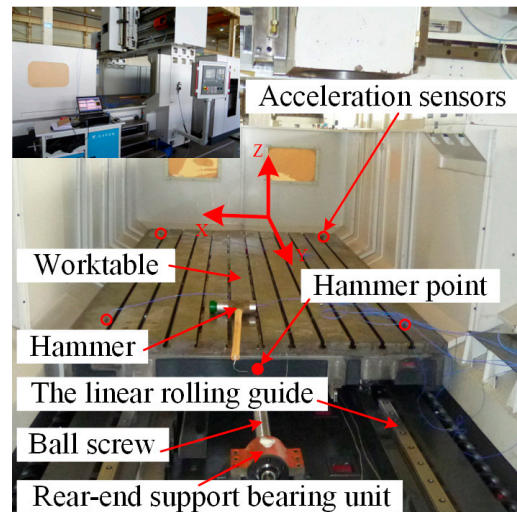


Figure 5. Dynamic measurement of the ball screw feed system.

Table 2. Detailed parameters of the acceleration sensors.

Type	Number	Sensitivity (mV/g)		
		X	Y	Z
356A66	SN 190783	9.99	9.85	10.33
	SN 190788	9.96	10.08	10.11
	SN 190789	9.95	9.78	9.82
	SN 190791	9.76	10.01	10.08

Further, the displacements (control strategy: linear acceleration \rightarrow uniform speed \rightarrow linear deceleration) of the worktable in the feed direction was measured using a laser interferometer system with a model of Renishaw Laser XL-80, as shown in Figure 6. The measurement mirror was fixed at the center of the worktable and the sampling frequency was set to 10,000 Hz. During testing, the worktable was restricted from moving in the range of $x_{vari} = [2.50\text{--}2.80]$ to reduce the influence of the variation in the stiffness matrix of the equivalent beam element. The feed system began to accelerate, at an acceleration of 0.50 m/s²; it maintained a uniform speed until the feed speed reached 150 mm/s, and then decelerated to a halt. The displacement response was acquired and stored using the data acquisition system of the Renishaw Laser XL-80.

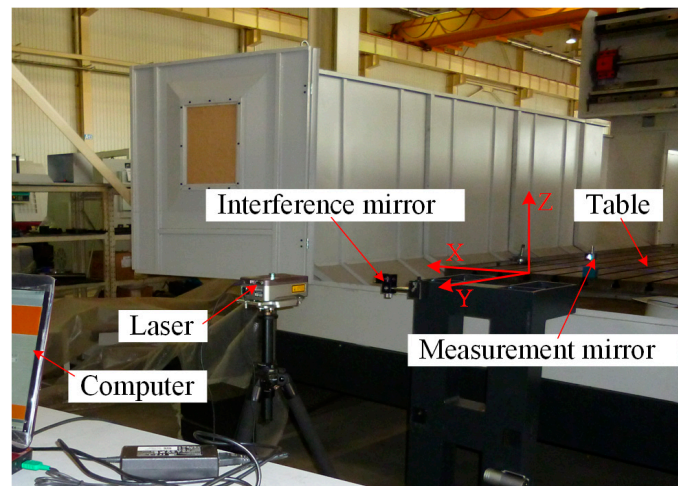


Figure 6. Displacement response measurement of the ball screw feed system in the feed direction.

4. Results and Discussion

4.1. Comparison of the Theoretical and Experimental Results Based on the Worktable Position

Figure 7 plots the average acceleration vibration response for the five tests. The mode shape corresponding to the marked natural frequency (32.0 Hz) in Figure 7 translates along the feed direction by LMS Test.Lab SCM05.

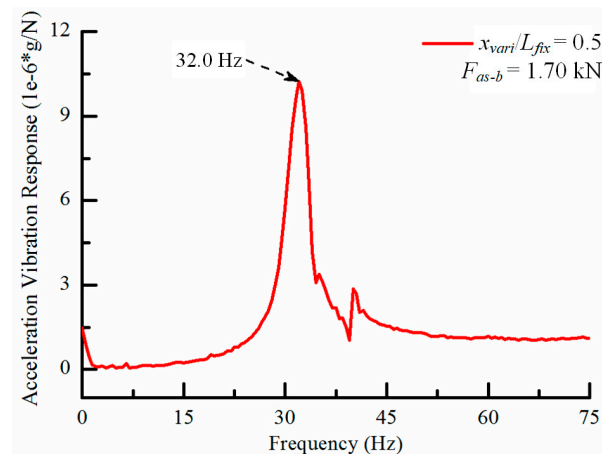


Figure 7. Frequency response of the feed system in the static state.

The undamped natural frequency of the system was calculated when the screw nut was located in the middle of the screw shaft, using the parameters in Table 1 and the equations in this study. Table 3 lists the theoretical (f_{the1}) and experimental results (f_{exp1}) of the natural frequency of the ball screw feed system. f_{the0} is the natural frequency of the ball screw feed system when the worktable is near the front-end support bearing unit ($x_{vari}/L_{fix} = 0.2$).

Table 3. Theoretical and experimental results of system frequency under static state.

	f_{the} (Hz)	f_{exp1} (Hz)	Error (%)
f_{the0}	35.9	32.0	12.19
f_{the1}	33.7	32.0	5.31

4.2. Comparison of the Theoretical and Experimental Results Based on the Feed Speed of the Worktable

The speed of the worktable in the feed direction was obtained by differentiating the displacement obtained by the Renishaw Laser XL-80, as shown in Figure 8. The acceleration of the worktable was 0.50 m/s^2 and the acceleration time was 0.3 s . Hence, the feed speed of the worktable was 150 mm/s . The electric current of the servo motor was measured using SigmaWinPlus when the feed speed of the worktable was 150 mm/s , as shown in Figure 9. The average value of positive uniform motion was -3.83 A and the average value of reversal uniform motion was 3.73 A ; therefore, the average value of the electric current was 3.78 A .

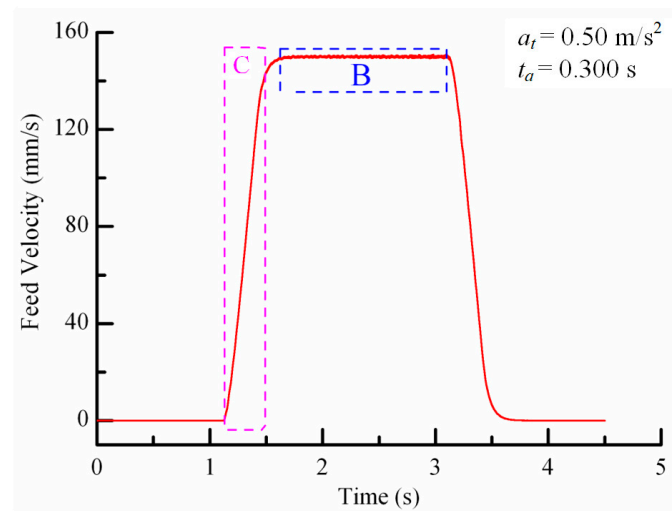


Figure 8. The speed of the worktable in the feed direction. B is the uniform velocity interval, C is the acceleration interval.

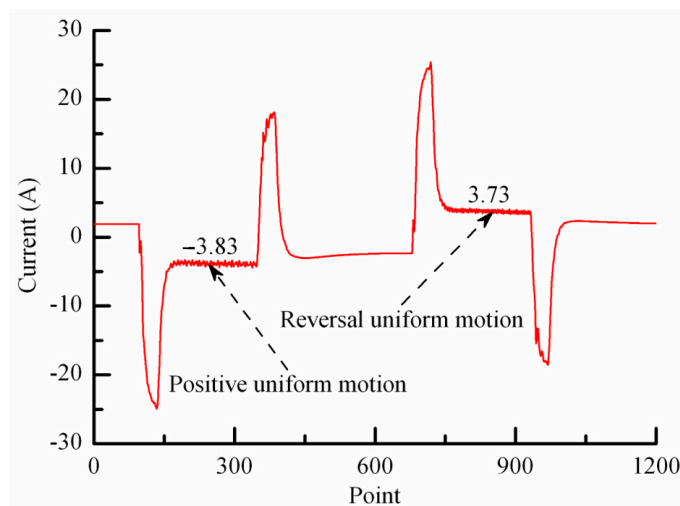


Figure 9. Electric current of the servo motor.

The friction force of the ball screw feed system is equal to the output-driven force of the servo motor when the worktable moves at a uniform speed. It can be expressed as follows [38,39]:

$$\begin{cases} T_{sm} \cdot \frac{2\pi}{p_{ss}} \cdot S_{dr} - f(v_t) = 0 \\ T_{sm} = k_t \cdot I_A \end{cases} \quad (15)$$

where

T_{sm} is the output-driven torque of the servo motor, S_{dr} is the reduction ratio of the servo motor, k_t is the torque constant of the servo motor, and I_A is the average current at uniform speed.

By substituting the friction forces calculated using Equation (15) at a feed speed of 150 mm/s and the detailed parameters in Table 1 into the equations in this study, the natural frequency of the ball screw feed system was calculated. After the Fourier transform of the velocity during the uniform speed process (region B) in Figure 8, the frequency response of the worktable was obtained, as shown in Figure 10. The sampling frequency was set to 10,000 Hz. A fitting method called Burg's method was used and the order was set to 300. Nfft was the point at which FFT was performed, and it was set to 10,240. Table 4 lists the theoretical (f_{the2}) and experimental results (f_{exp2}) of the ball screw feed system frequency at a feed speed of 150 mm/s.

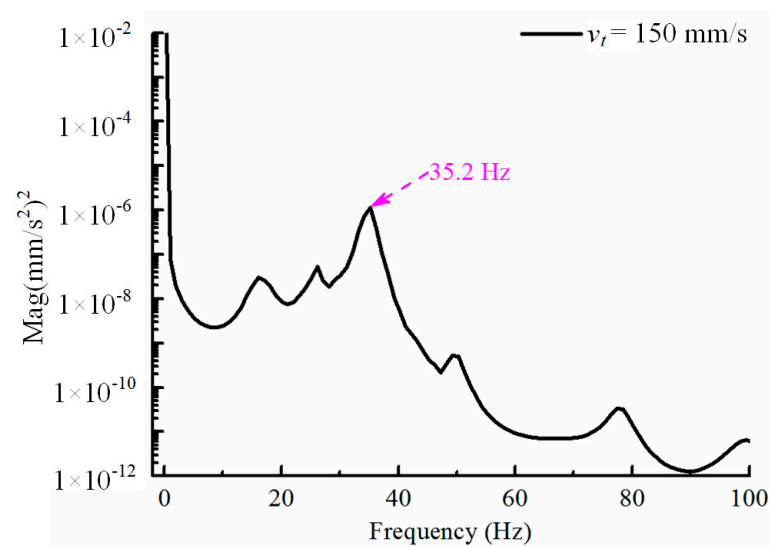


Figure 10. Frequency response of the system during the uniform speed process.

Table 4. Theoretical and experimental results of system frequency during the uniform speed process.

	f_{the} (Hz)	f_{exp2} (Hz)	Error (%)
f_{the1}	33.7	35.2	4.26
f_{the2}	34.1	35.2	3.13

4.3. Comparison of the Theoretical and Experimental Results Based on the Feed Acceleration of the Worktable

The ball screw feed system frequency was calculated by substituting the parameters in Table 1 and a feed acceleration of 0.50 m/s^2 into the equations in this study. After a Fourier transform of the speed during the acceleration process (region C), as shown in Figure 8, the frequency response of the ball screw feed system was obtained, as shown in Figure 11. Table 5 lists the theoretical (f_{the3}) and experimental results (f_{exp3}) of the ball screw feed system frequency. The sampling frequency was 10,000 Hz. A fitting method called Burg's method was used and the order was set to 300. The Nfft was set to 10,240.

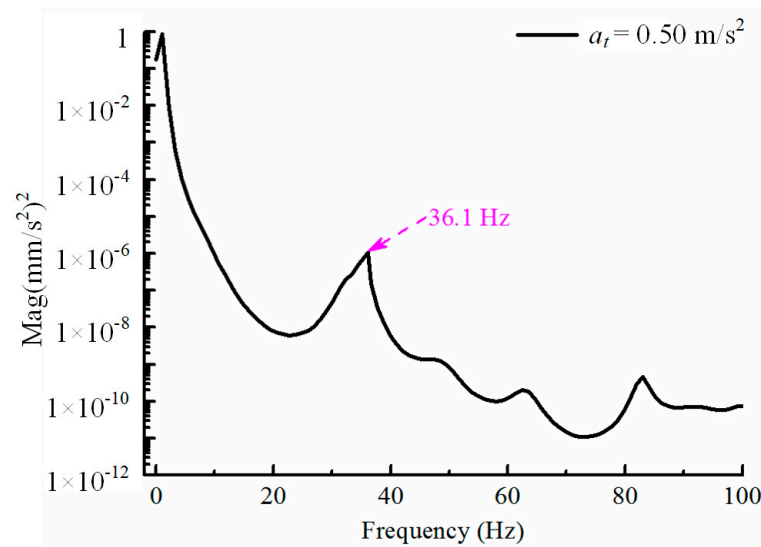


Figure 11. Frequency response of the system during the acceleration process.

Table 5. Theoretical and experimental results of system frequency during the acceleration process.

	f_{the} (Hz)	f_{exp3} (Hz)	Error (%)
f_{the1}	33.7	36.1	6.57
f_{the3}	34.7	36.1	3.88

In summary, the maximum error between the theoretical and experimental results of the ball screw feed system frequency was 5.31% when the running states were considered. However, the maximum error between the theoretical and experimental results of the ball screw feed system frequency was 12.19% when the influence of the running states was not considered. Therefore, the variable-coefficient dynamic modeling method proposed in this study, which is based on a ball screw feed system with a no-extra-load running state, has high accuracy. There is an evident error between the theoretical and experimental results. The primary reason for the error is that the influences of servo stiffness and non-dominant factors on transmission stiffness were neglected when calculating the transmission stiffness of the ball screw feed system. Furthermore, an accurate method to determine the value of the ball screw tension force and select the coefficient also affects the result of the transmission stiffness.

5. Conclusions

The main conclusions of this study are as follows:

(1) A variable-coefficient dynamic modeling method was proposed for a ball screw feed system, considering the influence of changes in the system's no-extra-load running state, such as feed position, feed speed, and feed acceleration. Based on Timoshenko beam elements with two nodes and four DOFs, an equivalent dynamic model of a ball screw feed system was developed using the hybrid element method.

(2) The expression for the equivalent axial stiffness of individual kinematic joints was derived by considering the influence of the ball screw feed system's feed speed/acceleration. The stiffness and mass of the screw shafts on both sides of the screw nut were calculated by considering the influence of the system's feed position and screw pitch. Consequently, the total stiffness and mass of the ball screw feed system in its no-extra-load were obtained in a running state and the natural frequency was analyzed. Finally, experiments on a ball screw feed system were performed to verify the accuracy of the proposed variable-coefficient dynamic model.

(3) The variable-coefficient dynamic modeling method proposed for a ball screw feed system in a no-extra-load running state has high accuracy. The relationship between the equivalent axial stiffness of the kinematic joints, the stiffness of the screw shafts, and the dynamic characteristics of the ball screw feed system with the system's no-extra-load running state can be used to guide the matching design of the kinematic joint stiffness of the system and assembly process.

6. Future Directions

In this paper, a variable-coefficient dynamic modeling method under a no-extra-load running state was established, calculated, and verified, and it has high accuracy. This paper's proposed model can not only provide a theoretical basis for the electromechanical integration and design/control of the ball screw feed system, but also improve the motion accuracy of the ball screw feed system. Finally, the machining accuracy and machining efficiency of the parts were increased. In the future, it will be necessary to study the electromechanical integration and control of the ball screw feed system in machine tools with variable dynamic characteristics. In addition, the influence of cutting force on the variable dynamics of the ball screw feed system needs to be studied.

Author Contributions: Conceptualization, H.Z. and H.L.; methodology, H.Z.; software, H.Z.; validation, H.Z. and J.Z.; formal analysis, H.Z.; investigation, H.Z.; resources, C.D.; data curation, H.Z.; writing—original draft preparation, H.Z.; writing—review and editing, J.Z. and Y.L.; visualization, H.Z.; supervision, H.Z.; project administration, D.L.; funding acquisition, H.Z., H.L. and J.Z. All authors have read and agreed to the published version of the manuscript.

Funding: This study was supported by the Key-Area Research and Development Program of Guangdong Province (Grant No. 2020B090927002), the National Natural Science Foundation of China (Grant No. 51975462), and the National Natural Science Funds of Shaanxi Province (Grant No. 2021JM-017, 2021JM-010).

Data Availability Statement: The datasets supporting this study's conclusions are included within the article.

Acknowledgments: The authors sincerely thank Professor Zhao of Xi'an Jiaotong University for his critical discussion and reading during the preparation of the manuscript.

Conflicts of Interest: The authors declare no competing financial interests.

References

1. Kim, M.S.; Chung, S.C. A systematic approach to design high-performance feed drive systems. *Int. J. Mach. Tools Manuf.* **2005**, *45*, 1421–1435. [[CrossRef](#)]
2. Altintas, Y.; Verl, A.; Brecher, C.; Uriarte, L.; Pritschow, G. Machine tool feed drives. *CIRP Ann.* **2011**, *60*, 779–796. [[CrossRef](#)]
3. Kamalzadeh, A.; Erkorkmaz, K. Compensation of Axial Vibrations in Ball Screw Drives. *CIRP Ann.* **2007**, *56*, 373–378. [[CrossRef](#)]
4. Erkorkmaz, K.; Kamalzadeh, A. High Bandwidth Control of Ball Screw Drives. *CIRP Ann.* **2006**, *55*, 393–398. [[CrossRef](#)]
5. Du, F.; Zhang, M.; Wang, Z.; Yu, C.; Feng, X.; Li, P. Identification and compensation of friction for a novel two-axis differential micro-feed system. *Mech. Syst. Signal Process.* **2018**, *106*, 453–465. [[CrossRef](#)]
6. Yang, X.; Lu, D.; Liu, H.; Zhao, W. Integrated modeling and analysis of the multiple electromechanical couplings for the direct driven feed system in machine tools. *Mech. Syst. Signal Process.* **2018**, *106*, 140–157. [[CrossRef](#)]
7. Kamalzadeh, A.; Erkorkmaz, K. Accurate tracking controller design for high-speed drives. *Int. J. Mach. Tools Manuf.* **2007**, *47*, 1393–1400. [[CrossRef](#)]
8. Toh, C. Vibration analysis in high speed rough and finish milling hardened steel. *J. Sound Vib.* **2004**, *278*, 101–115. [[CrossRef](#)]
9. Chanal, H.; Duc, E.; Ray, P. A study of the impact of machine tool structure on machining processes. *Int. J. Mach. Tools Manuf.* **2006**, *46*, 98–106. [[CrossRef](#)]
10. Law, M.; Altintas, Y.; Phani, A.S. Rapid evaluation and optimization of machine tools with position-dependent stability. *Int. J. Mach. Tools Manuf.* **2013**, *68*, 81–90. [[CrossRef](#)]
11. Law, M.; Ihlenfeldt, S.; Wabner, M.; Altintas, Y.; Neugebauer, R. Position-dependent dynamics and stability of serial-parallel kinematic machines. *CIRP Ann.* **2013**, *62*, 375–378. [[CrossRef](#)]
12. Weck, M.; Krüger, P.; Brecher, C. Limits for controller settings with electric linear direct drives. *Int. J. Mach. Tools Manuf.* **2001**, *41*, 65–88. [[CrossRef](#)]

13. Poignet, P.; Gautier, M.; Khalil, W. Modeling, control and simulation of high speed machine tool axes. In Proceedings of the Conference on Advanced Intelligent Mechatronics, Atlanta, GE, USA, 19–23 September 1999; pp. 617–622.
14. Okwudire, C.E.; Altintas, Y. Hybrid Modeling of Ball Screw Drives with Coupled Axial, Torsional, and Lateral Dynamics. *J. Mech. Des.* **2009**, *131*, 071002. [[CrossRef](#)]
15. Whalley, R.; Ebrahimi, M.; Abdul-Ameer, A.A. Machine Tool Axis Dynamics. *Proc. Inst. Mech. Eng. Part C J. Mech. Eng. Sci.* **2006**, *220*, 403–419. [[CrossRef](#)]
16. Zaeh, M.; Oertli, T.; Milberg, J. Finite Element Modelling of Ball Screw Feed Drive Systems. *CIRP Ann.* **2004**, *53*, 289–292. [[CrossRef](#)]
17. Law, M.; Phani, S.; Altintas, Y. Position-Dependent Multibody Dynamic Modeling of Machine Tools Based on Improved Reduced Order Models. *J. Manuf. Sci. Eng.* **2013**, *135*, 021008. [[CrossRef](#)]
18. Domblesky, J.P.; Feng, F. Two-dimensional and three-dimensional finite element models of external thread rolling. *J. Eng. Manuf.* **2002**, *216*, 507–517. [[CrossRef](#)]
19. Feng, G.-H.; Pan, Y.-L. Investigation of ball screw preload variation based on dynamic modeling of a preload adjustable feed-drive system and spectrum analysis of ball-nuts sensed vibration signals. *Int. J. Mach. Tools Manuf.* **2012**, *52*, 85–96. [[CrossRef](#)]
20. Zhou, Y.; Peng, F.Y.; Cao, X.H. Parameter sensitivity analysis of axial vibration for lead-screw feed drives with time-varying framework. *Mechanika* **2011**, *17*, 523–528. [[CrossRef](#)]
21. Mi, L.; Yin, G.-F.; Sun, M.-N.; Wang, X.-H. Effects of preloads on joints on dynamic stiffness of a whole machine tool structure. *J. Mech. Sci. Technol.* **2012**, *26*, 495–508. [[CrossRef](#)]
22. Feng, G.-H.; Pan, Y.-L. Establishing a cost-effective sensing system and signal processing method to diagnose preload levels of ball screws. *Mech. Syst. Signal Process.* **2012**, *28*, 78–88. [[CrossRef](#)]
23. Tsai, P.; Cheng, C.; Hwang, Y. Ball screw preload loss detection using ball pass frequency. *Mech. Syst. Signal Process.* **2014**, *48*, 77–91. [[CrossRef](#)]
24. Liu, H.; Zhang, J.; Xu, B.; Xu, X.; Zhao, W. Prediction of microstructure gradient distribution in machined surface induced by high speed machining through a coupled FE and CA approach. *Mater. Des.* **2020**, *196*, 109133. [[CrossRef](#)]
25. Liu, H.; Birembaux, H.; Ayed, Y.; Rossi, F.; Poulachon, G. Recent advances on cryogenic assistance in drilling operation: A critical review. *J. Manuf. Sci. Eng.* **2022**, *144*, 100801. [[CrossRef](#)]
26. Armstrong-Hélouvry, B.; Dupont, P.; De Wit, C.C. A survey of models, analysis tools and compensation methods for the control of machines with friction. *Automatica* **1994**, *30*, 1083–1138. [[CrossRef](#)]
27. Awrejcewicz, J.; Olejnik, P. Analysis of Dynamic Systems with Various Friction Laws. *Appl. Mech. Rev.* **2005**, *58*, 389–411. [[CrossRef](#)]
28. Reuss, M.; Dadalau, A.; Verl, A. Friction Variances of Linear Machine Tool Axes. *Procedia CIRP* **2012**, *4*, 115–119. [[CrossRef](#)]
29. Verl, A.; Frey, S. Correlation between feed velocity and preloading in ball screw drives. *CIRP Ann.* **2010**, *59*, 429–432. [[CrossRef](#)]
30. Zhang, J.; Zhang, H.; Du, C.; Zhao, W. Research on the dynamics of ball screw feed system with high acceleration. *Int. J. Mach. Tools Manuf.* **2016**, *111*, 9–16. [[CrossRef](#)]
31. Zhang, H.; Zhang, J.; Liu, H.; Liang, T.; Zhao, W. Dynamic modeling and analysis of the high-speed ball screw feed system. *Proc. Inst. Mech. Eng. Part B J. Eng. Manuf.* **2014**, *229*, 870–877. [[CrossRef](#)]
32. Lee, K.; Ibaraki, S.; Matsubara, A.; Kakino, Y.; Suzuki, Y.; Arai, S.; Braasch, J. A servo parameter tuning method for high-speed NC machine tools based on contouring error measurement. *WIT Trans. Eng. Sci.* **2003**, *44*, 12.
33. Frey, S.; Dadalau, A.; Verl, A. Expedient modeling of ball screw feed drives. *Prod. Eng.* **2012**, *6*, 205–211. [[CrossRef](#)]
34. Dhatt, G.; Touzot, G. *Finite Element Method*; John Wiley & Sons: Hoboken, NJ, USA, 2012.
35. Okamoto. *Design and Calculation of Ball Bearings*; Huang, Z.Q., Ed.; China Machine Press: Beijing, China, 2003.
36. Brewe, D.E.; Hamrock, B.J. Simplified solution for elliptical-contact deformation between two elastic solids. *J. Lubr. Technol.* **1977**, *99*, 485–487. [[CrossRef](#)]
37. Greenwood, J.A. Analysis of elliptical Hertzian contacts. *Tribol. Int.* **1997**, *30*, 235–237. [[CrossRef](#)]
38. He, W.X. *Permanent Magnet Motor*; China Power Press: Beijing, China, 2007.
39. Zirn, O. *Machine Tool Analysis: Modelling, Simulation and Control of Machine Tool Manipulators*; ETH Zurich, Institute of Machine Tools and Manufacturing: Zurich, Switzerland, 2008.

Disclaimer/Publisher's Note: The statements, opinions and data contained in all publications are solely those of the individual author(s) and contributor(s) and not of MDPI and/or the editor(s). MDPI and/or the editor(s) disclaim responsibility for any injury to people or property resulting from any ideas, methods, instructions or products referred to in the content.